Supporting Information

Brazelton et al. 10.1073/pnas.0905369107

SI Methods

Sample Names. Samples 1–4 in this study refer to DSV *Alvin* sample names 3881–1408, 3869–1404, 3869–1443, and 3876–1133, respectively. The NCBI Short Read Archive and names of 16S rRNA clones from previous studies (2) refer to samples 1–4 as LC1408, LC1404, LC1443, and LC1133, respectively. The VAMPS database (http://vamps.mbl.edu) identifies archaeal V6 tag sequences from this study as ICM_LCY_Av6 and bacterial V6 tag sequences as ICM_LCY_Bv6. Samples 1–4 are designated in VAMPS as LCY_0016_2003_05_16, LCY_0014_2003_05_04, LCY_0018_2003_05_04, and LCY_0012_2003_05_11, respectively, and bacterial V6 tag sequences as LCY_0005_2003_05_16, LCY_0003_2003_05_04, LCY_0007_2003_05_04, and LCY_0001_2003_05_11, respectively.

Sample Descriptions. Previous studies have used field observations to classify the LCHF chimney samples based on observable hydrothermal activity (where "active" samples are those egressing hydrothermal fluids and "inactive" chimneys have no apparent venting activity) (5). Active structures are typically very friable, porous (up to 50%) and are composed of a mix of aragonite ($CaCO_3$), brucite ($Mg(OH)_2$), and some calcite ($CaCO_3$) whereas inactive samples are typically more lithified and are composed of mostly aragonite and calcite (5). In this study, three samples from actively venting chimneys (samples 1–3) and one sample from an inactive chimney (sample 4) were selected to obtain a set of samples ranging from young to old and ranging from close to distant physical proximity. All samples were collected with DSV *Alvin* and stored in a closed "biobox" until shipboard retrieval. Samples 2 and 3 were collected on the same dive; other samples were collected on separate dives. Previously published microbiological and biochemical characteristics of these samples are summarized in Table S4.

Samples 2 (43 ± 23 yr) and 3 (128 ± 57 yr) are from a structure named "Marker C" and were located 20 cm apart (Fig. 1). Marker C is a ~50-cm-wide flange structure with several small (centimeters tall) chimneys growing on the top of the flange (Fig. 1). Sample 2 was collected from the front of the flange, and sample 3 was a small spire collected from the top (Fig. 1). Both structures were cream white with a reddish discoloration that remains unexplained (5). These chimneys were visibly venting, and the mixing of emitting fluids with ambient seawater created a temperature gradient of 9–70 °C from the interior of the flange outward. Porosity of the LCHF active chimneys ranges from <5% to 50% and is determined quantitatively using petrographic thin sections (5). Only one thin section of a sample in this study (sample 3) was made, which had a porosity of 33% (5). Samples representing earlier growth stages generally have higher porosities than samples representing later growth stages (5), so it is expected that samples 1–2 have >33% porosity, and sample 4 has <33% porosity. Visual examination of the samples supports this hypothesis, but quantitative measurements were not conducted.

Sample 1 (34.3 ± 8.1 yr) was collected from a site known as "Marker 3" or "Poseidon" (6). Poseidon is the landmark of the LCHF, towering 60 m above the seafloor, emitting fluids at temperatures of 55–88 °C (6). Sample 1 minerals appeared bright white in color, very friable, and not lithified. A mucilaginous substance, most likely a biofilm, coated the sample.

Sample 4 (1,245 ± 257 yr) was collected from a small spire growing from the basement rock on the eastern side of the field (Fig. 1). This structure was not visibly venting, although it was observed only once before sampling. It was gray in color, contained some biolithic material and had visible fluid flow channels, suggesting that some venting may have occurred in the recent past. Coral polyps were found on the exterior of the structure after recovery, which is typical of inactive chimneys at the LCHF (5). Temperature and chemistry conditions at this site were presumed to be that of ambient seawater, and no measurements were performed.

Fluid chemistry and temperature data from the chimneys at Marker 3 (sample 1) and Marker C (samples 2–3) do not show any obviously important differences (7, 8). The chimney at Marker 3 appears slightly hotter (88 °C maximum temperature compared with 70 °C maximum temperature), but the in situ temperature of the minerals collected in this study would have been determined by their distance from the fluid source. Sample 3 was most likely at a much cooler temperature than sample 2 because it was further from the chimney flange opening. Concentrations of H_2 and carbon species are highly similar at markers 3 and C (7, 8). Chimney mineralogy and ^{230}Th age, therefore, are expected to be much more important drivers of microbial community composition than are temperature and fluid chemistry, and the data presented in this study is consistent with that hypothesis.

U/Th Dating of Carbonate Chimneys. Numerous questions remain concerning the development, formation conditions, and microbial colonization of this novel hydrothermal system. Although previous work using radiocarbon techniques shows that hydrothermal activity has been ongoing for at least 30 kyr, modeling suggests that the field may be even older (9). The carbonate composition of the LCHF chimneys (5, 6) is amenable to both radiocarbon and U-series dating, allowing important constraints to be placed on the history of hydrothermal activity and the timescales over which the chimneys form. Uranium–thorium (^{238}U-^{234}U-^{230}Th-^{232}Th or U-Th or ^{230}Th) disequilibrium dating is a powerful geochronological tool used to date inorganic and biogenic materials ranging in age from modern to 600 kyr (10–12). In this study, four discrete chimney samples were dated using ^{238}U-^{234}U-^{232}Th-^{230}Th age dating techniques to compare these ages to the microbial community structure of coregistered samples.

For U-Th shore-based analyses, chimney subsamples were chemically prepared in the Minnesota Isotope Lab (MIL) using methods described in Edwards et al. (10) and Shen et al. (13). Approximately 0.2 g of carbonate was weighed in acid-cleaned Teflon beakers, dissolved in HNO_3, then spiked, as described by Chen et al. (14). After adding 5 drops of $HClO_4$, the samples were capped and heated for 4–6 h to remove organics and equilibrate the spike with the sample. Uranium and Th aliquots were separated using Fe coprecipitation and ion chromatography, dissolved in 1% HNO_3 + 0.005 N HF, and then stored in acid-cleaned plastic ICP vials. Procedural blanks were measured regularly. Three-month average values were 0.02 ± 0.01 pmol ^{238}U, 0.003 ± 0.003 pmol ^{232}Th, and 0.0006 ± 0.0005 fmol ^{230}Th.

All samples were analyzed on an ICP-SF-MS using methods described by Shen et al. (15). Data reduction was completed offline as described by Shen et al. (15). Ages were calculated iteratively as described by Edwards et al. (11) and Shen et al. (15). Values for decay constants λ_{230} (9.1577×10^{-6} yr^{-1}) and λ_{234} (2.8263×10^{-6} yr^{-1}) are from Cheng et al. (16) and λ_{238} (1.5513×10^{-10} yr^{-1}) is from Jaffey et al. (17). Measured errors of isotopic and concentration are given as 2 standard deviations of the mean ($2\sigma_m$) and age precisions are reported as 2 standard deviations (2σ). Ages of subsamples from the same large sample were highly similar, indicating that ages of the four samples in

this study are representative of the bulk material used for DNA extraction.

DNA Extraction from Carbonate Chimneys: Shipboard, subsamples of chimney material were frozen immediately at −80 °C and remained frozen until onshore analysis. DNA was extracted from carbonate chimney samples according to a protocol modified from previous reports (2, 18) and summarized here. After crushing a frozen carbonate sample with a sterile mortar and pestle, ≈0.25–0.5 g of chimney material were placed in a 2-mL microcentrifuge tube containing 250 μL of 2× buffer AE (200 mM Tris, 50 mM EDTA, 300 mM EGTA, 200 mM NaCl, pH 8) and 2 μg of poly-dIdC (Sigma-Aldrich) and incubated at 4 °C overnight to allow chelation of salts and binding of DNA to poly-dIdC. Between 36 and 72 replicate tubes were processed in parallel, and a ≈15-g quantity of carbonate minerals was processed for each sample. Proteinase K (final concentration 1.2 mg/mL) and 10 μL of 20% SDS were added to each tube before incubation at 37 °C for at most 30 min. An additional 150μL of 20% SDS and 500 μL of phenol:chloroform:isoamyl alcohol (25:24:1 ratio by volume) were added to each tube before centrifugation at 12,000 × *g* for 10 min. Supernatants were transferred to clean tubes for a second phenol:choloroform:isoamyl alcohol extraction. After centrifugation, supernatants were pooled into SnakeSkin dialysis tubing (Pierce) and dialyzed against 20 mM EGTA overnight at 4 °C. This large scale dialysis step proved to be very efficient in removing inorganic minerals and organic inhibitors. After dialysis, DNA was precipitated by adding 0.1 vol 3 M sodium acetate and 1 vol isopropanol and stored at −20 °C for 2–4 h. Pellets were collected by centrifugation at 16,000 × *g* for 20 min at 8 °C, washed once in 70% ethanol, dried in a vacuum centrifuge, and resuspended in TE (10 mM Tris, 1 mM EDTA, pH 8). Typical yield was ∼35 mg of DNA per g of carbonate chimney material.

Generation and Sequencing of V6 Amplicons. Archaeal and bacterial V6 amplicons were generated as previously described by Sogin et al. (19) and Huber et al. (20) and summarized here. PCR reactions used Platinum Taq HiFi polymerase (Invitrogen) to reduce errors introduced during amplification and involved the following cycling conditions: 94 °C for 2 min; 30 cycles of (94 °C for 30 s, 50 °C for 20 s, 72 °C for 1 min); and 72 °C for 2 min. A mixture of degenerate primers were used to maximize taxonomic coverage, as described by Huber et al. (20). Amplicon concentrations were quantitated with a BioAnalyzer 2100 (Agilent Technologies) and normalized among samples before sequencing. Amplicons from each sample were attached to beads and sequenced with a 454 Life Sciences GS20 pyrosequencer according to previously published protocols (19–21). Archaeal data were also generated with a 454 Life Sciences FLX pyrosequencer because the number of archaeal sequences generated by the GS20 were highly variable among samples. Sequences generated by both machines were pooled together to improve OTU clustering robustness, but comparisons of archaeal diversity among samples considered only FLX data. Sequences were screened for quality as recommended by Huse et al. (22). Specifically, all sequences satisfying any of the following criteria were not considered for further analysis: those with one or more Ns, those without an exact match to one of the forward primers, or those shorter than 50 nts after removal of primers. Automated taxonomic assignments of V6 tag sequences were performed by the GAST process, which compares V6 tags to a reference database of V6 regions from full-length 16S rRNA clones of known taxonomy (1). GAST requires two-thirds of the sequences of a given taxonomy to match the query tag sequence to make an assignment. If no taxonomic category fulfills the two-thirds rule, it is reported as "Unassigned" (Tables S2 and S3). As the taxonomy of uncultured organisms is inconsistently reported in GenBank, GAST is frequently unable to reliably assign taxonomy to groups of organisms without cultured representatives (e.g., ANME-1 in Table S2).

Estimation of Pyrosequencing Error. Each of the three extremely dominant sequence types representing the main archaeal groups was one member of a large, unexpectedly diverse pool of mostly rare sequences (Fig. 3*B*). For example, the four chimney samples contained 1,242 different V6 sequence types that were 3% distant or less from the dominant sequence, representing nearly half of all 2,635 sequence types identified in this study. An additional 530 sequence types were between 3% and 10% distant from the dominant sequence. Only 63 sequence types were more than 10% distant to the dominant sequence (together, these 1,835 sequence types clustered into the 534 OTUs displayed in Fig. 3). Similar patterns were seen with sequences related to the ANME-1 and Marine Group I clones: 403 different V6 sequence types are 3% distant or less from the dominant ANME-1 sequence, and 125 sequence types are 3% distant or less from the dominant Marine Group I sequence. Although pyrosequencing error may have generated some of the variant sequences within clusters, pyrosequencing error alone cannot account for all of the observed diversity. If the variant sequences within each major cluster are compared to that cluster's dominant sequence, a nucleotide substitution rate of 0.18% is calculated for the LCMS cluster, 0.08% for the ANME-1 cluster, and 0.76% for the Marine Group I cluster. (The much higher substitution rate for the Marine Group I cluster is due to the relatively high abundance of two variant sequences compared to the dominant sequence.) These values are much higher than the substitution rate of 0.03% attributed to pyrosequencing error of quality-screened tags by Huse et al. (22). Therefore, some of the most abundant variant sequences are extremely unlikely to be generated by pyrosequencing error and most likely represent genuine diversity within the phylogenetic group.

Determination of Variability Caused by Amplicon Generation and Sequencing. Because the three young chimney samples share the same dominant LCMS V6 sequence type, nearly all community differences in the presence/absence of OTUs among samples involve rare sequences. It is possible that differences involving rare sequences could be a trivial result because of inherent variability of the technique. We tested this possibility by generating and sequencing replicate amplicon libraries from the same DNA preparation of sample 1 to test whether the rare OTU membership was reproduced. Because the replicate sequencing runs were performed months apart, with independent amplifications from template, and on different pyrosequencing machines (454 Life Sciences GS20 and FLX), we consider this a very conservative test of replication. The GS20 replicate yielded 17,425 tag sequences and 343 OTUs. The FLX replicate yielded 16,260 tag sequences and 342 OTUs. The GS20 OTUs were randomly resampled down to 16,260 sequences, reducing the number of OTUs to 286. The Bray-Curtis similarity between the OTUs of the sample 1 replicates was high (89%) because of the nearly identical relative abundances of the most common OTUs. As expected, incomplete sampling of the amplicon library caused differences in the presence/absence of the many rare OTUs so that the Jaccard similarity between replicates was just 50%. (When sequence types represented by only one tag ("singletons") among all samples were removed from analysis before normalization and clustering, the Jaccard similarity improved to 73%.) Because the similarity between replicates was higher than the similarity between sample 1 and the other samples, the differences among samples are greater than that expected from the technique itself. A remarkable exception is the archaeal community similarity between samples 2 and 3 (95% Bray-Curtis, 56% Jaccard). The similarity was much higher than the similarity between sample 1 replicates, so the small differences between these samples may not reflect any natural variation. Therefore,

the archaeal communities of samples 2 and 3 can be considered identical. It should be noted, however, that samples 2 and 3 were both sequenced on the same machine (FLX), whereas sample 1 replicates were sequenced on different machines, so the actual experimental error between samples sequenced on the same machine is probably much lower than that represented by the sample 1 replicates.

Comparison with Clone Libraries. The nearly full-length sequences of 16S rRNA clones to which V6 tag sequences were compared have been previously published (2, 23). Global alignment sequence similarities between V6 tags and the corresponding region of 16S rRNA clones were calculated with MatGat (24). Phylogenetic trees of 16S rRNA clones were constructed with TreePuzzle, Version 5.2 (25) using default options and exact parameter estimation. GenBank accession numbers for sequences in Fig. 3 tree, from top to bottom: M59133, FJ791573, M59140, AY817738, AM746096, NC_010085, FJ795512, U51469. GenBank accession numbers for sequences in Fig. 5 tree, from top to bottom: AF329082, AF016046, DQ270609, FJ792098, AF013974, DQ270608, DQ270607, FJ792484, AJ404732, AB166731, L40810.

1. Huse SM, et al. (2008) Exploring microbial diversity and taxonomy using SSU rRNA hypervariable tag sequencing. *PLoS Genet* 4:e1000255.
2. Brazelton WJ, Schrenk MO, Kelley DS, Baross JA (2006) Methane- and sulfur-metabolizing microbial communities dominate the Lost City hydrothermal field ecosystem. *Appl Environ Microbiol* 72:6257–6270.
3. Schrenk MO, Kelley DS, Bolton SA, Baross JA (2004) Low archaeal diversity linked to subseafloor geochemical processes at the Lost City Hydrothermal Field, Mid-Atlantic Ridge. *Environ Microbiol* 6:1086–1095.
4. Bradley AS, Hayes JM, Summons RE (2009) Extraordinary ^{13}C enrichment of diether lipids at the Lost City Hydrothermal Field indicates a carbon-limited ecosystem. *Geochim Cosmochim Acta* 73:102–118.
5. Ludwig KA, Kelley DS, Butterfield DA, Nelson BK, Fruh-Green G (2006) Formation and evolution of carbonate chimneys at the Lost City Hydrothermal Field. *Geochim Cosmochim Acta* 70:3625–3645.
6. Kelley DS, et al. (2005) A serpentinite-hosted ecosystem: the Lost City hydrothermal field. *Science* 307:1428–1434.
7. Proskurowski G, Lilley MD, Kelley DS, Olson EJ (2006) Low temperature volatile production at the Lost City Hydrothermal Field, evidence from a hydrogen stable isotope geothermometer. *Chem Geol* 229:331–343.
8. Proskurowski G, et al. (2008) Abiogenic hydrocarbon production at Lost City Hydrothermal Field. *Science* 319:604–607.
9. Früh-Green GL, et al. (2003) 30,000 Years of hydrothermal activity at the Lost City Vent Field. *Science* 301:495–498.
10. Edwards RL, Chen JH, Wasserburg GJ (1986/1987) ^{238}U, ^{234}U, ^{230}TH, ^{232}TH systematics and the precise measurement of time over the past 500,000 years. *Earth Planet Sci Lett* 81:175–192.
11. Edwards RL, Chen JH, Ku TL, Wasserburg GJ (1987) Precise timing of the last interglacial period from mass-spectrometric determination of ^{230}TH in corals. *Science* 236:1547–1553.
12. Edwards RL, Gallup CD, Cheng H (2003) Uranium-series dating of marine and lacustrine carbonates. *Uranium-Series Geochemistry*, eds Bourdon S, Henderson G, Lundstrom CC, Turner SP (Mineralogical Society of America, New York), pp 363–405.
13. Shen C-C, et al. (2003) Measurement of attogram quantities of 231Pa in dissolved and particulate fractions of seawater by isotope dilution thermal ionization mass spectroscopy. *Anal Chem* 75:1075–1079.
14. Chen JH, Edwards RL, Wasserburg GJ (1986) ^{238}U, ^{234}U, and ^{232}Th in seawater. *Earth Planet Sci Lett* 80:241–251.
15. Shen C-C, et al. (2002) Uranium and thorium isotopic and concentration measurements by magnetic sector inductively coupled plasma mass spectrometry. *Chem Geol* 185:165–178.
16. Cheng H, et al. (2000) The half-lives of uranium-234 and thorium-230. *Chem Geol* 169: 17–33.
17. Jaffey AH, Flynn KF, Glendenin LE, Bentley WC, Essling AM (1971) Precision measurement of half-lives and specific activities of ^{235}U and ^{238}U. *Phys Rev C*4:1889–1906.
18. Barton HA, Taylor NM, Lubbers BR, Pemberton AC (2006) DNA extraction from low-biomass carbonate rock: An improved method with reduced contamination and the low-biomass contaminant database. *J Microbiol Methods* 66:21–31.
19. Sogin ML, et al. (2006) Microbial diversity in the deep sea and the underexplored "rare biosphere". *Proc Natl Acad Sci USA* 103:12115–12120.
20. Huber JA, et al. (2007) Microbial population structures in the deep marine biosphere. *Science* 5:97–100.
21. Margulies M, et al. (2005) Genome sequencing in microfabricated high-density picolitre reactors. *Nature* 437:376–380.
22. Huse SM, Huber JA, Morrison HG, Sogin ML, Welch DM (2007) Accuracy and quality of massively parallel DNA pyrosequencing. *Genome Biol* 8:R143.
23. Brazelton WJ, Baross JA (2009) Abundant transposases encoded by the metagenome of a hydrothermal chimney biofilm. *ISME J* 3:1420–1424.
24. Campanella JJ, Bitincka L, Smalley J (2003) MatGAT: An application that generates similarity/identity matrices using protein or DNA sequences. *BMC Bioinformatics* 4:29.
25. Schmidt HA, Strimmer K, Vingron M, von Haeseler A (2002) TREE-PUZZLE: Maximumlikelihood phylogenetic analysis using quartets and parallel computing. *Bioinformatics* 18:502–504.

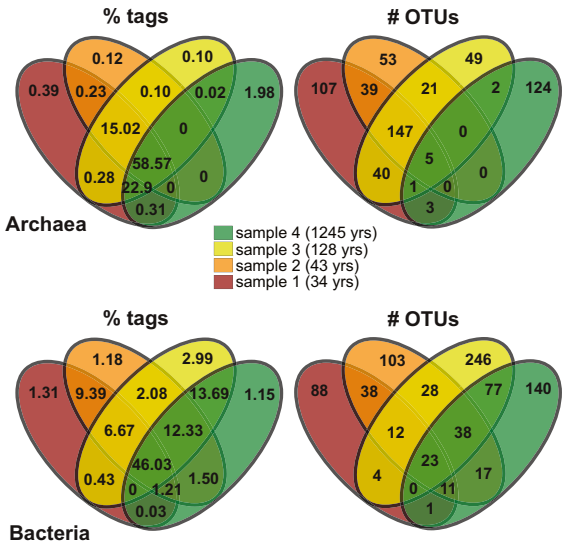

Fig. S1. Venn diagrams of archaeal and bacterial OTUs clustered with a 3% distance threshold showing the percentage of all tag sequences and the numbers of OTUs shared by the four chimney samples.

Archaeal V6 tag community similarities between samples

Bray-Curtis similarity	128 yrs	43 yrs	34 yrs
sample 4 (1245 yrs)	0.2	0.1	0.2
sample 3 (128 yrs)		95	87
sample 2 (43 yrs)			85
sample 1 (34 yrs)			

Jaccard similarity	128 yrs	43 yrs	34 yrs
sample 4 (1245 yrs)	1.9	1.1	1.5
sample 3 (128 yrs)		56	48
sample 2 (43 yrs)			50
sample 1 (34 yrs)			

Bacterial V6 tag community similarities between samples

Bray-Curtis similarity	128 yrs	43 yrs	34 yrs
sample 4 (1245 yrs)	36.1	37.7	12.1
sample 3 (128 yrs)		17.8	6.5
sample 2 (43 yrs)			45.0
sample 1 (34 yrs)			

Jaccard similarity	128 yrs	43 yrs	34 yrs
sample 4 (1245 yrs)	23.0	16.7	8.8
sample 3 (128 yrs)		17.4	8.3
sample 2 (43 yrs)			23.6
sample 1 (34 yrs)			

Fig. S2. Pairwise whole archaeal and bacterial community similarities between samples considering numbers of tag sequences in each OTU (Bray-Curtis) and considering only the presence/absence of each OTU (Jaccard).

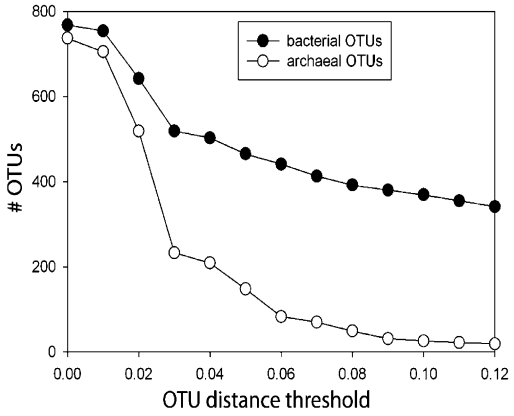

Fig. S3. Archaeal diversity is much lower than bacterial diversity at higher genetic distances. Number of archaeal and bacterial operational taxonomic units (OTUs) clustered at different pairwise distance thresholds are plotted for sample 2. At small distances, similar numbers of archaeal and bacterial OTUs were discovered. At large distances, very few archaeal OTUs were discovered, indicating very low diversity at high taxonomic levels (e.g., order, class, phylum).

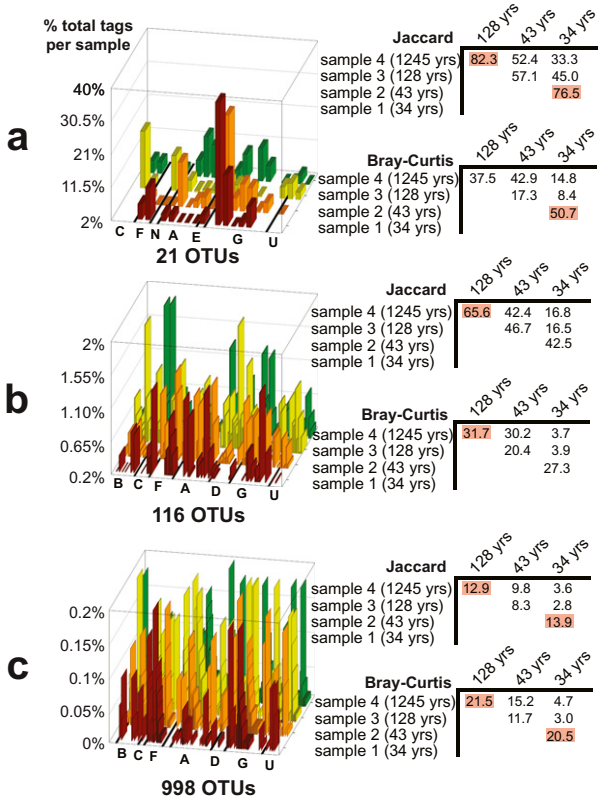

Fig. S4. Relative abundance of each bacterial OTU (clustered with a 3% distance threshold) in each of the four chimney samples and the resulting pairwise whole bacterial community similarities between samples. OTUs occurring at different relative abundance scales are displayed separately: (*A*) OTUs containing >2% of at least one sample's total tag sequences (*B*) OTUs containing 0.2% and 2% of a sample's total tag sequences (*C*) OTUs containing fewer than 0.2% of all samples' total tag sequences. Community similarities between samples remain fairly constant regardless of whether abundant or very rare OTUs are examined. The highest community similarities are typically between the two youngest samples and the two oldest samples (highlighted in red when they represent the two highest similarity values). OTUs are labeled according to their taxonomic assignment by GAST (1). A, *Alphaproteobacteria*; B, *Bacteroides*; C, *Chloroflexus*; D, *Deltaproteobacteria*; E, *Epsilonproteobacteria*; F, *Firmicutes*; G, *Gammaproteobacteria*; N, *Nitrospira*; U, Unassigned.

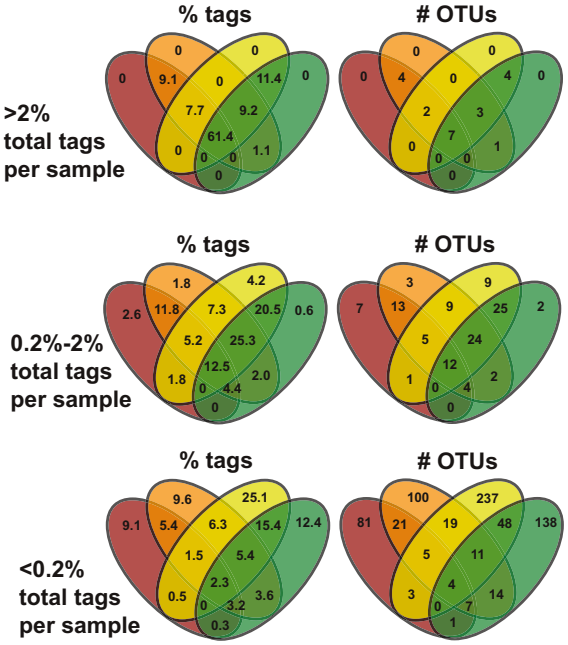

Fig. S5. Venn diagrams of bacterial OTUs (clustered with a 3% distance threshold) showing the percentage of all tag sequences and the numbers of OTUs shared by the four chimney samples. Separate Venn diagrams are shown for each of the relative abundance scales shown in Fig. S4.

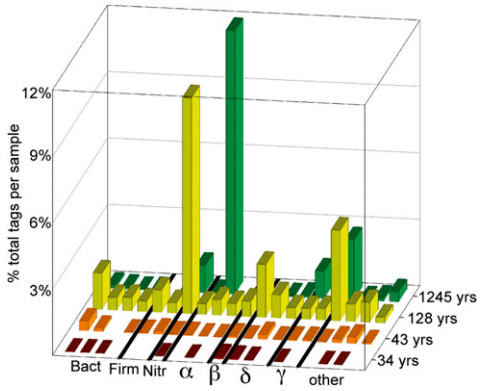

Fig. S6. Examples of OTUs that are dominant in old chimney samples and present but rare in young chimney samples. OTUs are labeled acccording to their taxonomic assignment. α, *Alphaproteobacteria*; β, *Betaproteobacteria*; Bact, *Bacteroides*; γ, *Gammaproteobacteria*; δ, *Deltaproteobacteria*; Firm, *Firmicutes*; Nitr, *Nitrospira*.

Table S1. Sequencing depth (as number of V6 tag sequences), observed number of OTUs (operational taxonomic units), richness estimators (ACE and Chao1), and Simpson's Reciprocal Index of diversity for all archaeal and bacterial OTUs in this study

	Archaea	Bacteria
V6 tag sequences	167,031	43,027
Unique sequence types	2,635 (1,163)	2,082
OTUs (3% distance)	817 (444)	1,135
ACE (3% distance)	980–1,024 (543–642)	2,203–2,362
Chao1 (3% distance)	943–1078 (524–641)	1,692–2,048
Simpson's Reciprocal Index (3% distance)	2.3 (2.3)	12.5
OTUs (10% distance)	116 (81)	653
ACE (10% distance)	142–191 (85–111)	1,215–1,294
Chao1 (10% distance)	130–246 (83–124)	922–1189
Simpson's Reciprocal Index (10% distance)	2.04 (2.04)	11.1

Values in parentheses are derived from randomly resampling the 167,031 archaeal tags down to 43,027 tags to compare archaeal diversity with bacterial diversity at equal sequencing efforts. The 167,031 archaeal tags includes 139,086 tags from the 454 Life Sciences FLX pyrosequencer and 27,945 tags from the 454 Life Sciences GS20 pyrosequencer.

Table S2. Numbers of archaeal tag sequences and OTUs clustered with a 3% distance threshold for the most frequently detected phyla, classes, and orders

			Sample 1 (34 yr)		Sample 2 (43 yr)		Sample 3 (128 yr)		Sample 4 (1,245 yr)	
Phylum	Class	Order	Tags	OTUs	Tags	OTUs	Tags	OTUs	Tags	OTUs
Crenarchaeota	MBGA	Unassigned	3	2	0	0	0	0	0	0
Crenarchaeota	MGI	Unassigned	5	3	0	0	0	0	0	0
Crenarchaeota	Thermoprotei	Unassigned	45	11	0	0	3	1	2	1
Crenarchaeota	Unassigned	Unassigned	259	27	0	0	10	5	7	4
Euryarchaeota	Methanomicrobia	Methanosarcinales	14,689	281	16,258	264	16,199	256	12	4
Euryarchaeota	Methanomicrobia	Methanosaetaceae	0	0	0	0	0	0	265	5
Euryarchaeota	Misc.		4	1	0	0	0	0	2	1
Euryarchaeota	Unassigned	Unassigned	53	15	0	0	2	1	15,935	116
Korarchaeota	Unassigned	Unassigned	2	1	0	0	0	0	0	0
Unassigned	Unassigned	Unassigned	1020	1	2	1	46	1	37	4
Archaea total			16,260	342	16,260	265	16,260	265	16,260	135

Taxonomies were assigned with the GAST algorithm (1). Numbers of tag sequences have been normalized down to a total of 16,260 sequences per sample by random resampling after OTU clustering. Prenormalized total numbers of tag sequences were 16,260 (sample 1); 32,345 (sample 2); 25,471 (sample 3); and 21,983 (sample 4). Most of the OTUs labeled 'LCMS' in Fig. 3 of the main text were assigned to order *Methanosarcinales*; most ANME-1 OTUs were assigned to *Euryarchaeota* unassigned; and most MGI OTUs were assigned to "*Crenarchaeota* unassigned" or "unassigned."

Table S3. Numbers of bacterial tag sequences and OTUs clustered with a 3% distance threshold for the most frequently detected phyla, classes, and orders

			Sample 1 (34 yr)		Sample 2 (43 yr)		Sample 3 (128 yr)		Sample 4 (1,245 yr)	
Phylum	Class	Order	Tags	OTUs	Tags	OTUs	Tags	OTUs	Tags	OTUs
Acidobacteria	Acidobacteria	Acidobacteriales	0	0	0	0	10	7	3	2
Acidobacteria	Unassigned	Unassigned	0	0	0	0	1	1	0	0
Actinobacteria	Actinobactera	Misc.	0	0	2	2	12	5	23	9
Actinobacteria	Unassigned	Unassigned	0	0	0	0	3	1	14	2
Bacteroidetes	Bacteroidia	Bacteroidales	0	0	0	0	3	1	1	1
Bacteroidetes	Flavobacteria	Flavobacteriales	27	7	103	18	301	37	40	10
Bacteroidetes	Sphingobacteria	Sphingobacteriales	42	4	29	8	39	21	11	9
Bacteroidetes	Unassigned	Unassigned	36	2	11	4	48	12	3	1
BRC1	Unassigned	Unassigned	0	0	0	0	89	5	163	9
Chloroflexi	Anaerolineae	Unassigned	2	1	0	0	0	0	0	0
Chloroflexi	Caldilineae	Caldilineales	1	1	3	1	11	1	1	1
Chloroflexi	Dehalococcoidetes	Unassigned	0	0	0	0	1,083	17	518	8
Deferribacteres	Deferribacteres	Deferribacterales	5	1	0	0	7	2	1	1
Deferribacteres	Unassigned	Unassigned	0	0	0	0	1	1	0	0
Deinococcus-Thermus	Deinococci	Misc.	31	4	0	0	0	0	0	0
Firmicutes	Bacilli	Misc.	0	0	1	1	2	1	0	0
Firmicutes	Clostridia	Misc.	1,073	42	426	31	228	21	57	9
Nitrospira	Nitrospira	Nitrospirales	0	0	3	1	601	8	83	3
OD1	Unassigned	Unassigned	0	0	8	2	62	10	10	5
Proteobacteria	Alphaproteobacteria	Misc.	15	3	24	10	14	9	9	7
Proteobacteria	Alphaproteobacteria	Rhizobiales	121	3	15	6	64	6	45	13
Proteobacteria	Alphaproteobacteria	Rhodobacterales	273	19	1294	40	545	39	2146	50
Proteobacteria	Alphaproteobacteria	Unassigned	102	9	108	7	149	25	140	16
Proteobacteria	Betaproteobacteria	Burkholderiales	15	3	11	5	72	6	13	7
Proteobacteria	Betaproteobacteria	Misc.	0	0	3	1	6	3	0	0
Proteobacteria	Deltaproteobacteria	Desulfobacterales	5	2	52	9	379	30	96	13
Proteobacteria	Deltaproteobacteria	Desulfovibrionales	15	5	3	3	2	2	1	1
Proteobacteria	Deltaproteobacteria	Misc.	0	0	14	6	18	11	14	9
Proteobacteria	Epsilonproteobacteria	Campylobacterales	158	9	29	9	36	11	21	4
Proteobacteria	Epsilonproteobacteria	Nautiliales	0	0	0	0	1	1	0	0
Proteobacteria	Gammaproteobacteria	Methylococcales	0	0	54	3	233	7	221	6
Proteobacteria	Gammaproteobacteria	Thiotrichales	3,483	42	3,122	56	371	21	1,429	30
Proteobacteria	Gammaproteobacteria	Misc.	114	10	153	21	459	42	192	32
Proteobacteria	Unassigned	Unassigned	2	2	52	11	325	14	182	15
Tenericutes	Mollicutes	Acholeplasmatales	0	0	1	1	35	4	5	2
Thermomicrobia	Unassigned	Unassigned	2	1	3	1	23	1	2	2
Misc. assigned*			42	6	7	7	63	23	21	11
Unassigned			3	1	36	6	271	22	102	19
Bacteria total			5,567	177	5,567	270	5,567	428	5,567	307

Taxonomies were assigned with the GAST algorithm (1). Numbers of tag sequences have been normalized down to a total of 5,567 sequences per sample by random resampling after OTU clustering. Prenormalized total numbers of tag sequences were 21,582 (sample 1); 5,567 (sample 2); 7,162 (sample 3); and 8,716 (sample 4). All of the *Thiomicrospira* sequences in Fig. 6 of the main text are included under *Thiotrichales* here. Most of the "misc" *Clostridia* sequences have high sequence similarity to previously published *Desulfotomaculum*-like clones (2).

*Misc. assigned includes: *Chlamydiae, Chlorobi, Cyanobacteria, Fibrobacteres, Fusobacteria, Gemmatimonadetes, Lentisphaerae, Planctomycetes, Spirochaetes, Thermotogae*, TM7, and *Verrucomicrobia*

Table S4. Previously published microbiological and biochemical characteristics of the four carbonate chimney samples

	Cells·g^{-1} dry weight*	Archaea†	Bacteria†	LCMS†	Total organic carbon, %	$\delta^{13}C_{toc}$, ‰ vs. VPDB
Sample 1 (3,881–1,408)	2.0×10^8	25	14	18	ND	ND
Sample 2 (3,869–1,404)	$1{,}200 \times 10^8$	41	8	32	0.20	−7.8
Sample 3 (3,869–1,443)	$1{,}600 \times 10^8$	38	10	21	ND	ND
Sample 4 (3,876–1,133)	1.6×10^8	24	19	12	0.15	−16.3

Cell densities and proportions of phylogenetic groups are from Schrenk et al. (3). Organic carbon concentrations and isotopic measurements are from Bradley et al. (4).

*Determined by DAPI staining.

†Percentage of DAPI-stained cells detected by FISH probe specific to each group.

Some data also from: Schrenk MO. (2005) Exploring the diversity and physiological significance of attached microorganisms in rock-hosted deep-sea hydrothermal environments. University of Washington doctoral dissertation.